

Research Article

Simultaneous Control of NO_x-Soot by Substitutions of Ag and K on Perovskite (LaMnO₃) Catalyst

Ganesh Chandra Dhal^{1*}, Subhashish Dey¹, Devendra Mohan¹, R. Prasad²

¹Department of Civil Engineering, IIT (BHU) Varanasi, Uttar Pradesh, India

²Department of Chemical Engineering and Technology, IIT (BHU) Varanasi, Uttar Pradesh, India

Received: 19th July 2017; Revised: 8th September 2017; Accepted: 8th September 2017;

Available online: 22nd January 2018; Published regularly: 2nd April 2018

Abstract

The different Ag and K substituted perovskite catalysts including base catalyst were LaMnO₃ by the solid state method and the diesel soot was prepared in the laboratory. Their structures and physico-chemical properties were characterized by X-ray diffraction (XRD), BET, SEM, H₂-TPR, and XPS techniques. The Ag Substituted at A-site perovskite structured catalysts are more active than other type of catalysts for the simultaneous soot-NO_x reaction, When Ag and K are simultaneously introduced into LaMnO₃ catalyst, soot combustion is largely accelerated, with the temperature (T_m) for maximal soot conversion lowered by at least 50 °C, moreover, NO_x reduction by soot is also facilitated. The high activity of La_{0.65}Ag_{0.35}MnO₃ perovskite catalyst is attributed to presence of metallic silver in the catalyst. The activity order of Ag doped LaMnO₃ is as follows La_{0.65}Ag_{0.35}MnO₃ > La_{0.65}Ag_{0.2}MnO₃ > La_{0.65}Ag_{0.4}MnO₃ > La_{0.65}Ag_{0.1}MnO₃. The dual substitution of silver and potassium in place of La in LaMnO₃ gives better activity than only silver doped catalyst. In a series of La_{0.65}Ag_xK_{1-x}MnO₃, the optimum substitution amount of K is for $x=0.25$. The single and doubled substituted perovskite catalyst proved to be effective in the simultaneous removal of NO_x and soot particulate, the two prevalent pollutants in diesel exhaust gases in the temperature range 350-480 °C. Copyright © 2018 BCREC Group. All rights reserved

Keywords: Perovskite catalysts; Simultaneous removal of NO_x and diesel soot; solid state method

How to Cite: Dhal, G.C., Dey, S., Mohan, D., Prasad, R. (2018). Simultaneous Control of NO_x-Soot by Substitutions of Ag and K on Perovskite (LaMnO₃) Catalyst. *Bulletin of Chemical Reaction Engineering & Catalysis*, 13 (1): 144-154 (doi:10.9767/bcrec.13.1.1152.144-154)

Permalink/DOI: <https://doi.org/10.9767/bcrec.13.1.1152.144-154>

1. Introduction

Over the last decades, with growing urbanization and increasing the numbers of automobiles, the increase of road traffic, and exhaust gas emissions started to cause were accompanied by a negative impact on the air quality, the environment, and human health. Mostly the diesel engines are more popular due to low cost

and high engine efficiency [1-3]. The main contaminants emitted by this type of engine are NO_x and soot particles. The NO_x formation by the internal combustion due the high ignition temperature is well understood but the formation soot is more complicated and difficult to examine [4,5]. It is a big challenge to control these two pollutants with the fulfillment of exhausts emission regulation without affecting the fuel economy of diesel engines [6,7].

Catalytic combustion can be carried out in a wider range of air-to-fuel ratios, capable of con-

* Corresponding Author.

E-mail: ganesh.dhal@gmail.com (Dhal, G.C.)

trolling NO_x and soot simultaneously [8-10]. It is big a challenge to develop suitable catalytic materials for application in the field of environmentally hazardous emissions safety. Perovskite-type oxides perform to be a promising alternative to noble metal catalysts in perspective of their low cost, thermochemical stability at relatively high temperatures and catalytic activity [11]. Many perovskite-oxides can be considered, given that the general ABO₃ structure, where a rare-earth metal A and a transition metal B are in the +3 oxidation state is compatible with a number of different combinations [12]. Any A and/or B replacement with non-equivalent ions is likely to stabilize an unusual oxidation state or a mixed valence state in the transition metal ions in the B site, thus changing the electronic properties and therefore modifying the catalytic performance of the so-formed perovskite [13,15].

Previous studies on LaCr_{1-x}Mg_xO₃ and LaMn_{1-x}Mg_xO₃ [15] have shown a promoting effect of the substitution on the catalytic activity of the resulting perovskite. The objective of the present paper is to enhance the catalytic activities of LaMnO₃ catalyst for simultaneous control of Soot and NO_x in diesel engine by double substitution with Ag and K which bring down the catalytic activity of LaMnO₃ within the exhaust temperature (>500 °C).

2. Materials and Methods

2.1 Catalyst preparation

Various catalysts including the base catalyst LaMnO₃ were prepared by the solid-state method as reported by Wang *et al.* [16]. The precursor salts like La(NO₃)₃·6H₂O, and Mn(CH₃COO)₂·4H₂O powders were mixed in a stoichiometric ratio and grinded continuously for 20 min in a mortar to make a uniform mixture. Compared with the theoretical weight, 20 % excessive NaOH was added into the mortar and solid was grinded thoroughly to react completely. Then the as-synthesized sample was washed with deionized water by the filter to remove the extra NaOH. The solid product was collected from the filter and dried at 100 °C for 24 h, followed by calcination at 600 °C for 10 h in air. After grinding the calcined product, the catalyst powder was obtained.

2.2 Soot preparation

The soot was prepared by partial combustion of commercial diesel (HP) in a lamp with the limited supply of air and collected on the inner walls of an inverted beaker Figure 1. The

soot was collected from the recipient walls and then dried in an oven overnight at 120 °C [17].

2.3 Catalyst characterization

X-ray measurement of the catalyst was carried out using Rigaku Ultima IV X-ray diffractometer (Germany) for phase identification. The patterns were run with Cu-Kα radiation at 40 kV and 40 mA. The mean crystallite size (*d*) of the phase was calculated from the line broadening of the most intense reflection using the Scherrer in Equation (1).

$$d = \frac{0.89 \lambda}{\beta \cos \theta} \quad (1)$$

Where *d* is the mean crystallite diameter, 0.89 is the Scherrer constant, *l* is the X-ray wave length (1.54056 Å), and *b* the effective line width of the observed X-ray reflection, calculated by the expression $b^2 = B^2 - b_0^2$ (where *B* is the full width at half maximum (FWHM), *b* is the instrumental broadening) determined through the FWHM of the X-ray reflection at 2θ of crystalline SiO₂.

Fourier transform infrared spectroscopy (FTIR) of the prepared catalyst was recorded in the range of 400–4000 cm⁻¹ on Shimadzu 8400 FTIR spectrometer with KBr pellets at room temperature. Specific surface area (SSA) measurements were performed using Micromeritics ASAP 2020 analyzer by physical adsorption of N₂ at the temperature of liquid nitrogen (196 °C), using the BET method in the standard pressure range of 0.05–.30 *P/P*₀.

Scanning electron micrographs (SEM) and SEM-EDX were recorded on Zeiss EVO 18 scanning electron microscope (SEM) instru-

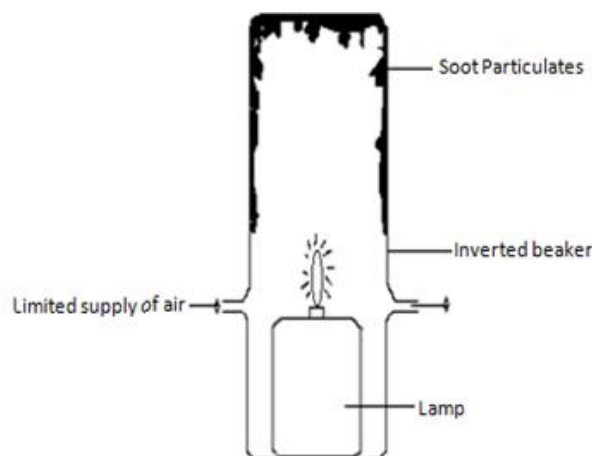


Figure 1. Preparation of soot

ment. An accelerating voltage of 15 kV and magnification of 1000X was applied. Particle size analysis of the samples were measured using the Laser diffraction (Helium-Neon Laser, 5 Milliwatt maximum output) based particle size analyser (ANKERSMID, CIS-50, U.S.A.) relies on the fact that particles passing through a laser beam will scatter light at an angle that is directly related to their size.

X-ray photoelectron spectroscopy (XPS) was used to monitor the surface compositions and chemical states of the constituent elements and performed on an Amicus spectrometer equipped with Mg K α X-ray radiation. For typical analysis, the source was operated at a voltage of 15 kV and current of 12 mA. The binding energy scale was calibrated by setting the main C 1s line of adventitious impurities at 284.7 eV, giving an uncertainty in peak positions of 0.2 eV.

Brunauer-Emmett-Teller (BET) surface areas were measured at -196 °C using a Micromeritics ASAP 2020 analyzer in present case. Samples were degassed at 300 °C under vacuum prior to the measurement. The calculation was performed using the adsorption data in the relative pressure (P/P_0) range from 0.05 to 0.35, and the total volumes were determined from the amounts adsorbed at $P/P_0 = 0.99$.

Temperature programmed reduction (TPR) analysis was carried out on a Micromeriticsplus chemisorb 2705 instrument and NO reduction was measured by Portable NO Analyzers (TECHNOVATION, series-89). Simultaneously measured the both soot oxidation and NO reduction in single flow conditions: NO-Ar mixture flow rate = 30 mL.min⁻¹, oxygen flow rate = 10 mL.min⁻¹, air flow rate = 60 mL.min⁻¹, 0.2-

0.5 g sample weight (soot/cat=1/20), heating rate 10 °C min⁻¹, and temperature range from 150-600 °C.

2.4 Experimental setup

The details of the experimental setup for the simultaneous reduction of NO_x and Soot to measure activities has shown in Figure 2. The reactant and product gases were analyzed by an on-line gas chromatograph (GC) equipped with Porapak Q-column, methanizer and FID detector for LPG, CO and CO₂ and TCD detector for O₂ and N₂ analysis.

The Gas Chromatograph (NUCON, Series 5765) is modular, Solid State Instrument designed for a variety of analytical and non-analytical applications. It comprise of the basic unit to which a broad range of optional modules may be added. Options available permit isothermal or temperature programmed operation, use of thermal conductivity or flame ionization detectors, syringe or valve sample introduction.

A large oven with a removal front opening door is standard. Each heated zone- Injectors, Detectors, Column oven is insulated to minimize heat transfer between zones, the temperature of each one of which can be controlled and read independently. Flow, pressure controls of the carrier gas, air are housed on the top towards the back of the oven. Top mounted injectors allow vertical sample injection.

2.5 Reaction conditions

The catalytic activities of the prepared catalyst samples were evaluated by passing NO and air over the soot – catalyst mixture. The

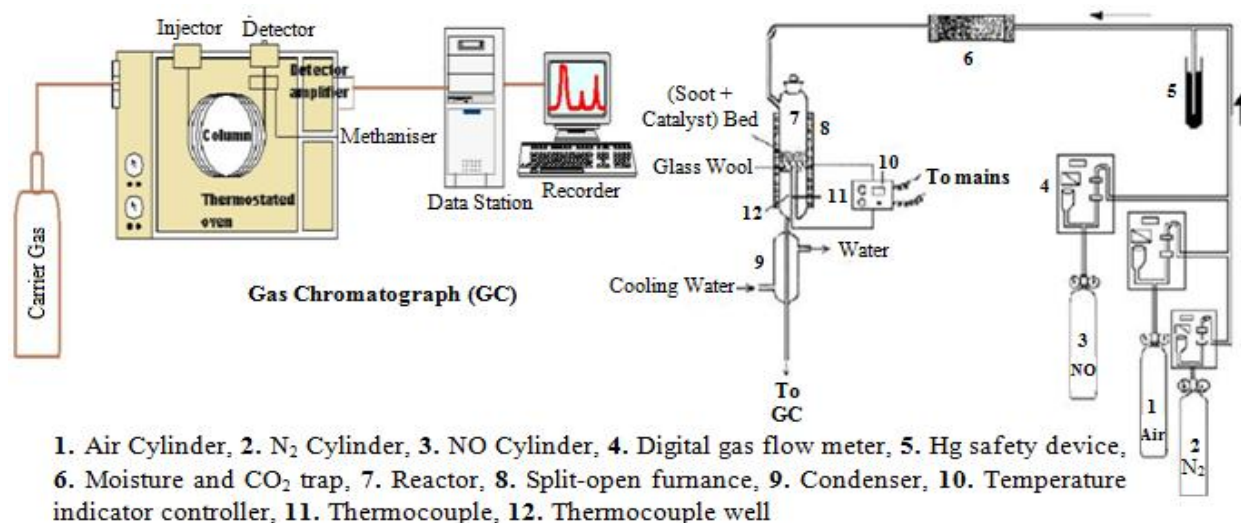


Figure 2. Reactor setup for the simultaneous reduction of NO_x and Soot

reaction temperature varied from 150 °C to 600 °C. Soot particulates (lab synthesized) and catalyst was carefully mixed, in the weight ratio of 1/20 for a “loose” contact and “tight” contact as well, between the soot particulates and the catalyst, and then placed onto the glass wool bed in the reactor. The catalytic activity was evaluated by recording the variation in NO ppm being observed in the NO analyser and evolution of CO₂ gas as a result of soot combustion by analyzing the outlet gasses with the help of GC as discussed previously [21-26].

2.6 Parameters for activity measurement

The activity parameters considered for soot-oxidation were light-off-temperature characteristics defined as follows: (1). Soot-ignition temperature (T_i); (2). Temperature for 50% soot oxidation (T_{50}); (3). Temperature for complete soot oxidation (T_{100}); (4). Temperature for maximum rate of soot oxidation known as peak temperature (T_p); (5). Percent soot conversion (% X_{soot}).

The parameters considered for NO reduction were as follows: (1). Temperature for maximum NO reduction (T_{max-NO}); and (2). Percent NO

conversion (% X_{NO}). The NO and soot conversions were calculated by formulas (Equations (2-3)), respectively.

$$\% \text{ NO Conversion, } X_{NO} = \frac{C_{NO \text{ inlet}} - C_{NO \text{ outlet}}}{C_{NO \text{ inlet}}} \times 100 \quad (2)$$

$$\% \text{ Soot Conversion, } X_{Soot} = \frac{\sum_{k=0}^n \text{Area } CO_2 \times \Delta T_K}{\sum_{k=0}^{\infty} \text{Area } CO_2 \times \Delta T_K} \times 100 \quad (3)$$

3. Result and Discussion

3.1 Scanning Electron Microscope (SEM) analysis

To study the morphology of the catalysts, SEM micrographs of La_{0.65}Ag_{0.35}MnO₃ and soot were taken at different magnifications (500X, 1000X, 2000X, 5000X, 10000X, 20000X). The micrographs of La_{0.65}Ag_{0.35}MnO₃ are shown in the Figure 3(a) and (b) the lower magnification images showed that the prepared catalyst surface consists of lumped and spherical grains and exhibits largely open porous structure. The pores are indicated by the black spots. The higher magnification images Figure 3(c) and (d) showed that the single aggregate particle consists of numerous smaller particles with

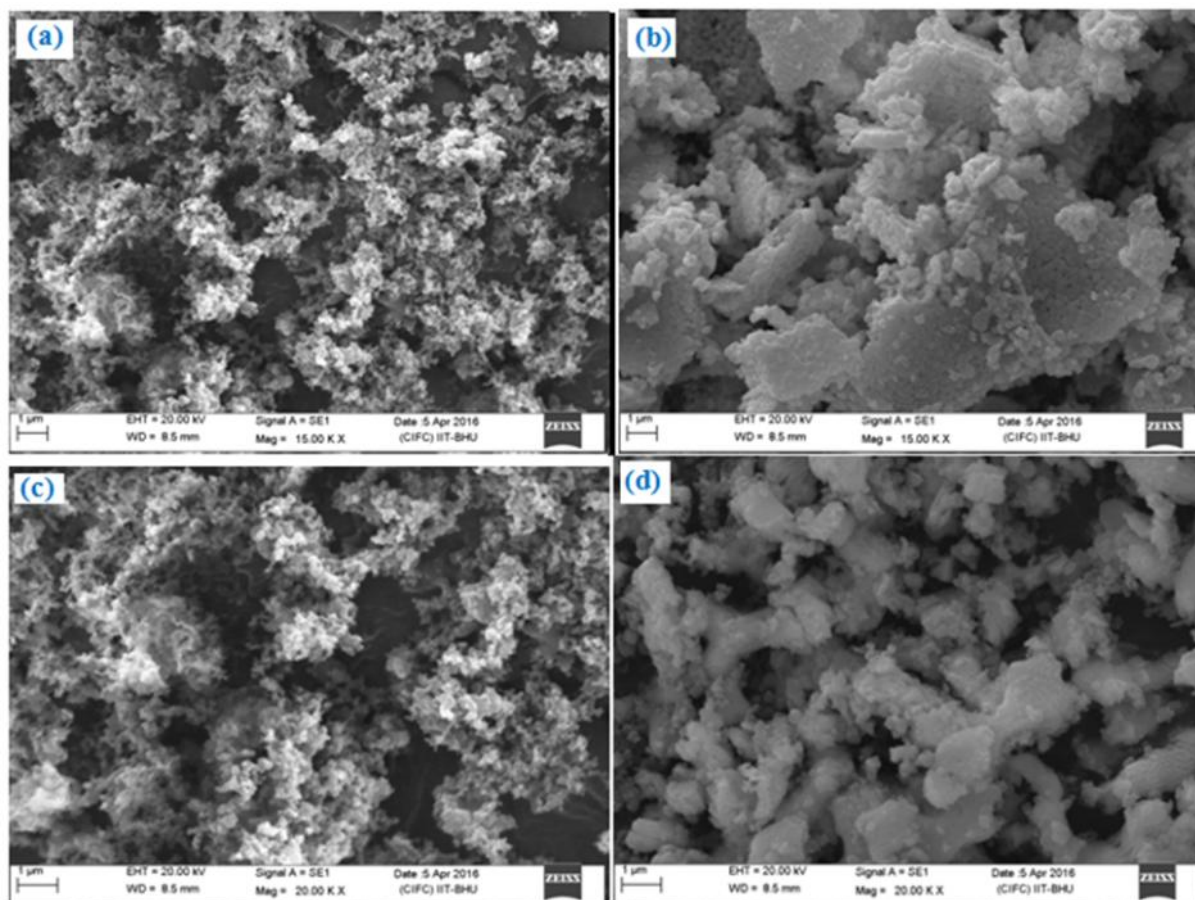


Figure 3. SEM micrographs of soot and La_{0.65}Ag_{0.35}MnO₃ catalyst

highly intra-particle porosity. XRD analysis confirmed the presence of metallic silver as a discrete phase which is indicated by the bright spots in the SEM micrographs. The distribution of silver is however not very uniform. This might be attributed to the manual mixing during the catalyst preparation. Although the pore distribution is not uniform, the catalyst has high BET surface area which is favorable for the activity of the catalyst.

3.2 X-Ray Diffraction (XRD) analysis

The XRD patterns of various perovskite type prepared catalysts were studied and detailed description is given below. Crystallite size of the samples prepared by various methods is summarized in Table 1.

3.2.1 XRD pattern of LaMnO₃ and La_{0.65}Ag_{0.35}MnO₃

X-Ray diffractograms of LaMnO₃ and La_{0.65}Ag_{0.35}MnO₃ are shown in Figure 4. The 2-theta values for LaMnO₃ shows that the catalyst has rhombohedral perovskite phase (JCPDS 89-8775). On comparing the XRD pattern of La_{0.65}Ag_{0.35}MnO₃ with that of LaMnO₃, it was found that the perovskite structure re-

mained intact even after the substitution of silver at A-site. However, some additional peaks at 2θ values of 38.116° (111), 44.300° (200), 64.445° (220) and 77.393° (311) were also obtained which confirms the presence of metallic Ag (JCPDS 65-2871).

3.2.2 XRD pattern of La_{0.65}Ag_{0.35}MnO₃ and La_{0.65}Ag_{0.1}K_{0.25}MnO₃

From the XRD diffractogram comparison of La_{0.65}Ag_{0.35}MnO₃ and La_{0.65}Ag_{0.1}K_{0.25}MnO₃ is shown in Figure 5, it is clear that intensity of the peaks corresponding to metallic silver in La_{0.65}Ag_{0.35}MnO₃ has decreased and three additional peaks corresponding to KMnO₄ at 39.509° (411), K₂MnO₄ at 48.593° (131) and 55.477° (125) were obtained.

3.3 Surface area and textural properties

Low temperature (-196 °C) nitrogen adsorption isotherms were used for the determination of the textural properties of the catalysts synthesized. The textural parameters including BET surface area, total pore volume and pore diameter of the catalysts are summarized in Table 2. The typical isotherm of La_{0.65}Ag_{0.35}MnO₃ is shown in Figure 6, which is

Table 1. Crystallite size of various catalyst prepared by Scherrer's method

S.N.	Catalyst	Crystallite size (Å)
1.	LaMnO ₃	3.5945
2.	La _{0.65} Ag _{0.35} MnO ₃	3.9318
3.	La _{0.65} Ag _{0.1} K _{0.25} MnO ₃	3.7467

Table 2. Textural characterization of prepared catalyst

S.N.	Catalyst	Surface Area (m ² /g)	Pore Volume (cm ³ /g)	Average pore Diameter (Å)
1.	LaMnO ₃	10.8995	0.009066	46.71
2.	La _{0.65} Ag _{0.35} MnO ₃	13.6920	0.010912	48.21
3.	La _{0.65} Ag _{0.1} K _{0.25} MnO ₃	10.5762	0.007579	49.64

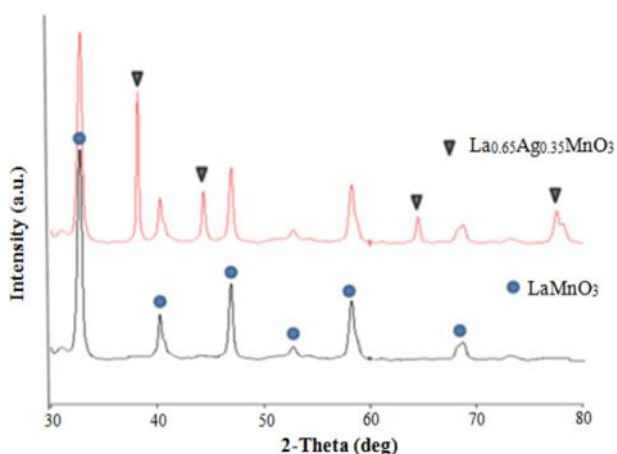


Figure 4. XRD patterns of LaMnO₃ and La_{0.65}Ag_{0.35}MnO₃

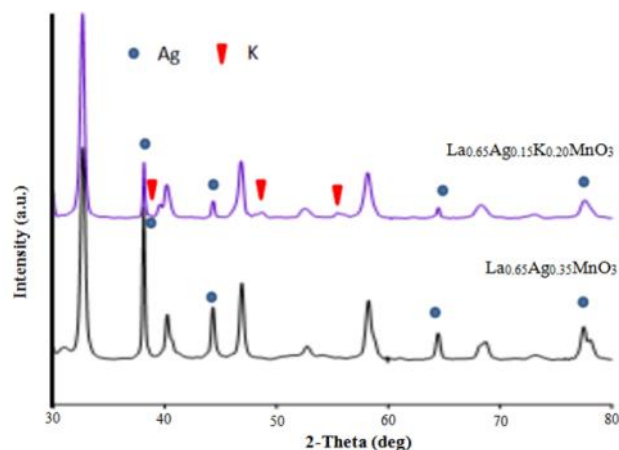


Figure 5. XRD patterns of La_{0.65}Ag_{0.15}K_{0.2}MnO₃ and La_{0.65}Ag_{0.35}MnO₃

of type IV of IUPAC classification 1984. This type of isotherm occurs on porous adsorbent with pores in the range of 1.5-100 nm. The average pore diameter obtained by BET analysis suggests that catalyst was mesoporous. The initial part of the isotherm is attributed to monolayer adsorption. At higher pressures the slope shows increased uptake of adsorbate as the pores become filled, inflection point typically occurs near the completion of the first monolayer. In the mesoporous materials, due to larger pores, the greater number of molecules interacts with each other and displays better catalytic activity. Hysteresis loops occur at low relative pressures (around 0.4) and the area within the loop is very small suggesting open cylindrical pores of the catalyst.

The BET surface area and pore volume of $\text{La}_{0.65}\text{Ag}_{0.35}\text{MnO}_3$ are ($13.6920 \text{ m}^2\text{g}^{-1}$) and ($0.010912 \text{ cm}^3\text{g}^{-1}$) which is higher than the above prepared catalysts. It is believed that the exothermic heat of decomposition of the precursor at $300 \text{ }^\circ\text{C}$ in stagnant-air does not dissipate quickly, causing rise in local temperature, sub-

sequently sintering the freshly generated nanocrystallites. Meanwhile, during flowing air the heat of decomposition under same conditions dissipate to some extent preventing little sintering.

3.4 Catalytic activity measurement

As per the literature review the substituted perovskite type of catalyst are found to be highly active for the simultaneous soot- NO_x reduction. As discussed before in perovskite structure (ABO_3), A and B sites have their individual influence on the catalyst properties. The A site metal has a strong effect on stability whereas the B-site is responsible for the catalytic activity. Generally, the A site is lanthanum and the B-site is a transition metal like Co, Mn, Cu, etc. Catalysts with Mn at B-site have been reported with considerable activity for the simultaneous soot- NO_x reaction [20]. Also, as reported by Wang *et al.* [16], silver substitution at A site enhances the activity of LaMnO_3 by lowering the soot ignition temperature (T_i), the temperature for maximum soot combustion (T_p) and increasing the % NO_x reduction.

Researchers have also reported that alkali metal substitution at A site improves the activity of the catalyst. Thus, the study of the silver and alkali substituted catalyst has been performed in this work. For further enhancement in activity, the B-site substitution with various transition metals viz. Fe, Co, Cu, and Ni is done and comparative study on the activity parameters was performed. Thus, the prepared catalysts were tested for their activity and the results obtained are tabulated as shown in Table 3.

3.5. Effect of A-site substitution

3.5.1 Silver substitution

The metallic Ag can efficiently adsorb NO and O_2 , and oxidize NO to NO_2 and as NO_2 being a better oxidizer for soot than NO or O_2 , en-

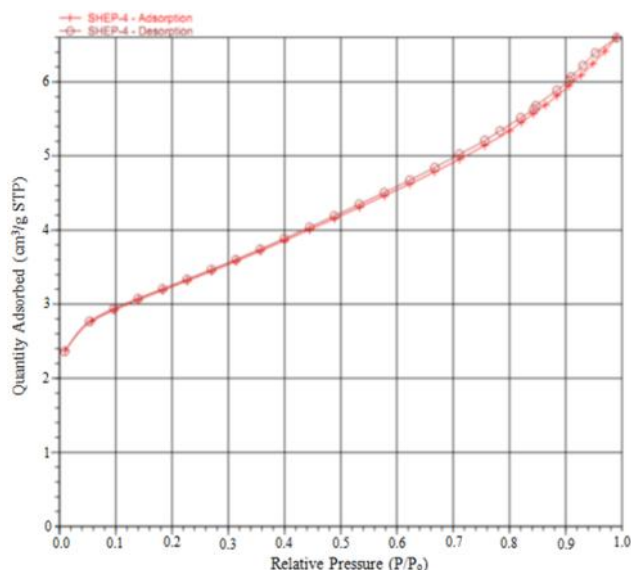


Figure 6. Nitrogen adsorption- desorption isotherm for the $\text{La}_{0.65}\text{Ag}_{0.35}\text{MnO}_3$ catalyst

Table 3. Different catalysts activity

S. No.	Catalyst	Soot oxidation				NO reduction	
		T_i ($^\circ\text{C}$)	T_{50} ($^\circ\text{C}$)	T_{100} ($^\circ\text{C}$)	T_p ($^\circ\text{C}$)	$T_{\text{max-NO}}$ ($^\circ\text{C}$)	Conversion (%)
1.	LaMnO_3	205	307.2	533	380	386	45.3
2.	$\text{La}_{0.65}\text{Ag}_{0.35}\text{MnO}_3$	152	256.5	490	300	301	53.2
3.	$\text{La}_{0.65}\text{Ag}_{0.1}\text{K}_{0.25}\text{MnO}_3$	135	328.27	452	355	368	64.4

hances the activity for both soot-oxidation and NO_x reduction [27,28]. Also, the O_2 -TPD and H_2 -TPR study performed by Ag-substituted over LaMnO_3 confirmed the presence of mass oxygen vacancies and over-stoichiometric oxygen due to substitution [29-32]. Silver substitution enhances the oxidation state of Mn^{+3} ion and creates oxygen vacancies. It has confirmed that the oxygen vacancy concentration directly relates to adsorption of NO which is significant to the activation of NO molecule and hence the catalytic activity [33].

The experimental results are in accordance with the above-stated theories. From the Table 3, it can be easily deduced that the silver substituted $\text{La}_{0.65}\text{Ag}_{0.35}\text{MnO}_3$ has better catalyst activity than pure LaMnO_3 . Both T_p and $T_{\text{max-NO}}$ occurred at a temperature lower than that for the pure LaMnO_3 confirming $\text{La}_{0.65}\text{Ag}_{0.35}\text{MnO}_3$ a better catalyst (Figures 7 and 8). The presence of metallic Ag is confirmed by XRD analysis. The soot ignition temperature was found to be reduced by 50°C as compared to the unsubstituted LaMnO_3 with an increase of 17% in the NO reduction efficiency of the catalyst. Also, the soot oxidation is more rapid for Ag-substituted catalyst as compared to unsubstituted one. The temperature values for maximum soot oxidation and maximum NO reduction matched perfectly confirming the simultaneous soot- NO_x reaction.

BET surface area results also confirmed an increase in the specific surface area of the substituted catalyst i.e. more surface area is available for adsorption of the reactants. Thus, we can conclude that addition of silver to LaMnO_3 catalyst is beneficial for simultaneous soot- NO_x reaction.

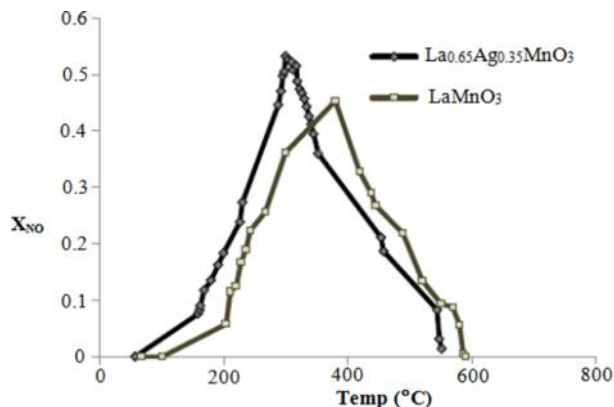


Figure 7. Effect of Ag substitution on NO conversion (X_{NO}) in LaMnO_3 catalyst

3.5.2 Optimization of the amount of silver substitution

To optimize the amount of silver substitution at the A-site, the catalyst with varying compositions with respect to the A-site component were prepared with general formula $\text{La}_{1-x}\text{Ag}_x\text{MnO}_3$ where $x = 0.15, 0.25, 0.35,$ and 0.4 . The activities of the four catalysts for soot oxidation were recorded as shown in Figure 9, it is clear that the catalyst $\text{La}_{1-x}\text{Ag}_x\text{MnO}_3$ with $x = 0.35$ has lowest soot ignition temperature. Also, the soot oxidation completed below 500°C , unlike the other catalysts. It is clear that initially with the increase in the value of x up to 0.35 , the soot ignition temperature and the temperature for complete soot oxidation decreased but for the value of x greater than 0.35 , both the temperatures started increasing. The NO_x reduction curve in Figure 10 also shows that the catalyst with $x = 0.35$ has the highest NO_x reduction of 53.28% at 300°C only. Thus,

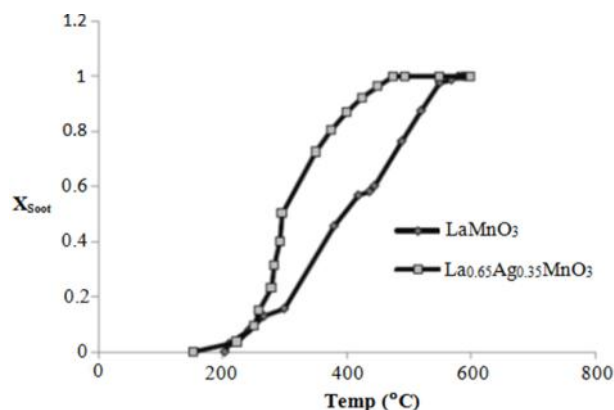


Figure 8. Effect of Ag substitution on soot conversion (X_{Soot}) in LaMnO_3 catalyst

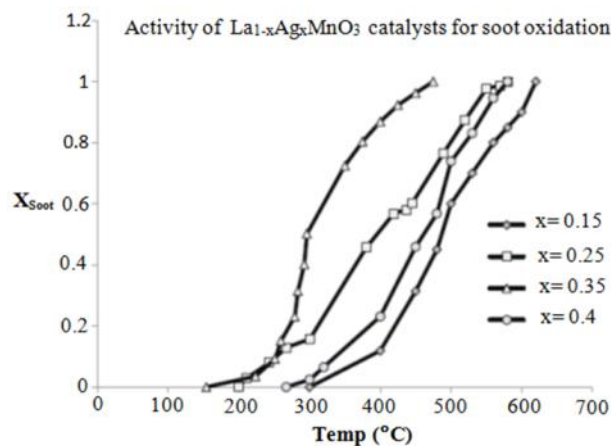


Figure 9. Effect of varying amount of Ag substitution on soot conversion in $\text{La}_{1-x}\text{Ag}_x\text{MnO}_3$ catalyst

it can be concluded that $\text{La}_{0.65}\text{Ag}_{0.35}\text{MnO}_3$ is the optimum substitution concentration for the LaMnO_3 catalyst.

3.5.3 Alkali metal substitution

The partial substitution of A-site cation (La^{+3}) with lower valence potassium ions (K^+) increases the oxidation state of the B-site ion (i.e. Mn^{+3} to Mn^{+4}) or creates some oxygen vacancies to maintain the electrical neutrality [33-37]. The higher oxidation state ions are usually known to possess higher catalytic activity whereas the oxygen vacancies enhance the surface oxygen and oxygen mobility in the lattice and both of these factors lead to increase in the catalytic activity [38-41].

Thus, a catalyst $\text{La}_{0.65}\text{Ag}_{0.1}\text{K}_{0.25}\text{MnO}_3$ with the combination of Ag and K ion at the A-site was prepared. The simultaneous effect of Ag and K substitutions at the A-site on soot conversion and NO reduction is shown in Figures

11 and 12, respectively. Dual substitution of Ag and K improved the activity for the soot oxidation considerably from the LaMnO_3 . Although the soot ignition started a little early (i.e. 130 °C) for the dually substituted catalyst, the trend of both $\text{La}_{0.65}\text{Ag}_{0.1}\text{K}_{0.25}\text{MnO}_3$ and $\text{La}_{0.65}\text{Ag}_{0.35}\text{MnO}_3$ for soot oxidation was quite similar. For soot conversion, the catalytic activity can be rated as:

$$\text{La}_{0.65}\text{Ag}_{0.1}\text{K}_{0.25}\text{MnO}_3 \approx \text{La}_{0.65}\text{Ag}_{0.35}\text{MnO}_3 > \text{LaMnO}_3$$

It is evident from the Figure 13 that simultaneous substitution of Ag and K at the A-site of LaMnO_3 catalyst improved the NO conversion considerably from 45% to 64%. Also, the NO conversion of the catalyst is better than only Ag-substituted catalyst (53.28%). However, the temperature for maximum NO conversion was higher for K-substituted catalyst than the only Ag-substituted catalyst. Thus, the selectivity of the catalyst for NO reduction can be given as follows: $\text{La}_{0.65}\text{Ag}_{0.1}\text{K}_{0.25}\text{MnO}_3 > \text{La}_{0.65}\text{Ag}_{0.35}\text{MnO}_3 > \text{LaMnO}_3$

Optimization of the amount of alkali metal substitution in order to optimize the amount of

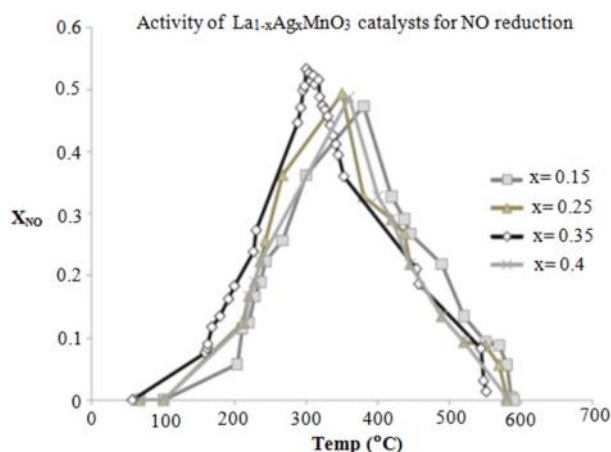


Figure 10. Effect of varying amount of Ag substitution on NO conversion in $\text{La}_{1-x}\text{Ag}_x\text{MnO}_3$ catalyst

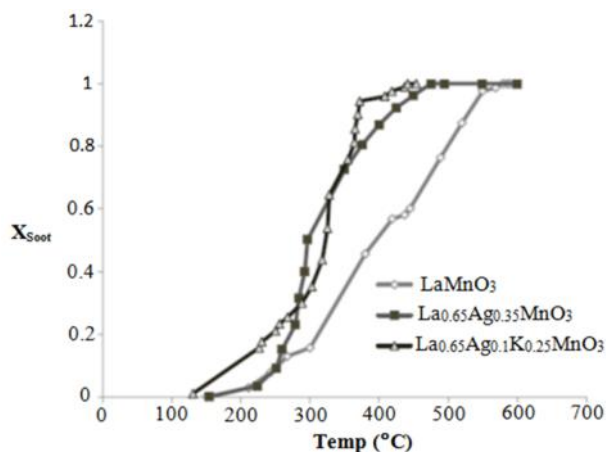


Figure 11. Effect of Ag and K substitutions on soot conversion in LaMnO_3 catalyst

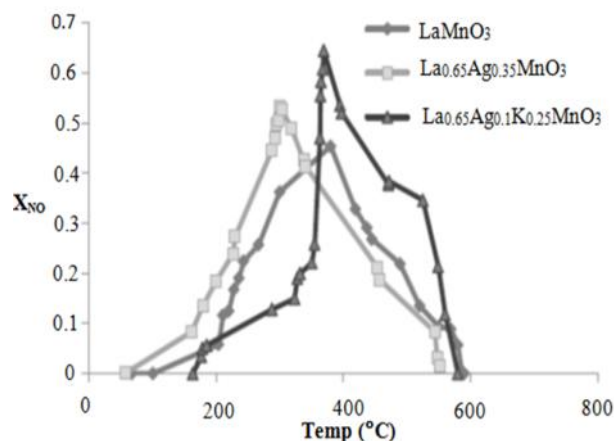


Figure 12. Effect of Ag and K substitutions on NO conversion in LaMnO_3 catalyst

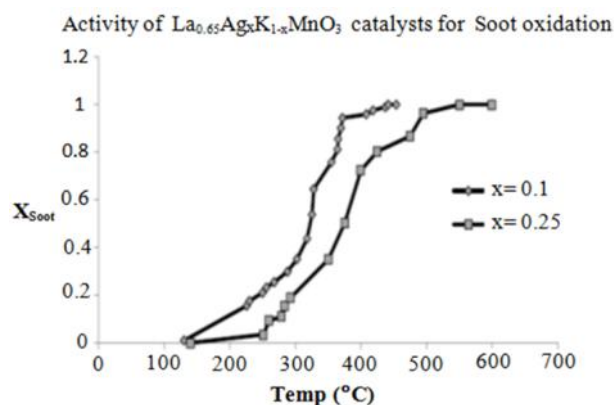


Figure 13. Effect of varying amount of K on soot conversion in $\text{La}_{0.65}\text{Ag}_x\text{K}_{1-x}\text{MnO}_3$ catalyst

potash substitution in the place of silver, $\text{La}_{0.65}\text{Ag}_x\text{K}_{1-x}\text{MnO}_3$ catalysts with $x = 0.1, 0.2$ were prepared. Experiments were conducted to evaluate the activity of the catalyst for simultaneous soot- NO_x reaction as shown in Figures 13 and 14. From the figures it can be easily inferred that the catalyst with $x = 0.1$ has better activity than the catalyst with $x = 0.2$ as it starts the soot ignition at lower temperature (130 °C) and completes the reaction much faster (454 °C) than the other catalyst with $T_i = 140$ °C. Also, the %NO reduction is higher for the catalyst with $x = 0.1$ than the other. The catalyst with $x = 0.2$ displayed better behavior, with $T_i = 140$ °C and 52.35% X_{NO} than the LaMnO_3 catalyst with $T_i = 204$ °C and 45.34% X_{NO} confirming that addition of potassium has the positive effect on the catalyst activity. The comparative study is summarized in Table 4.

4. Conclusion

In conclusion, the series of LaMnO_3 catalysts were prepared by the solid-state method presented superior NO_x reduction activity and soot oxidation activity over a relatively wide temperature range (350-480 °C). Moreover, the $\text{La}_{0.65}\text{Ag}_{0.35}\text{MnO}_3$ catalyst displayed highest conversion activity, which is very promising for practical applications in simultaneously controlling NO_x and Soot emissions. The Silver substitution at A-site of LaMnO_3 catalyst improves the catalytic activity for simultaneous soot- NO_x reduction. The high activity of $\text{La}_{0.65}\text{Ag}_{0.3}\text{MnO}_3$ perovskite catalyst is attributed to the presence of metallic silver in the catalyst. The activity order of Ag-doped LaMnO_3 is as follows: $\text{La}_{0.65}\text{Ag}_{0.35}\text{MnO}_3 > \text{La}_{0.65}\text{Ag}_{0.25}\text{MnO}_3 > \text{La}_{0.65}\text{Ag}_{0.45}\text{MnO}_3 > \text{La}_{0.65}\text{Ag}_{0.15}\text{MnO}_3$. Dual substitution of silver and potassium in place of La in LaMnO_3 gives

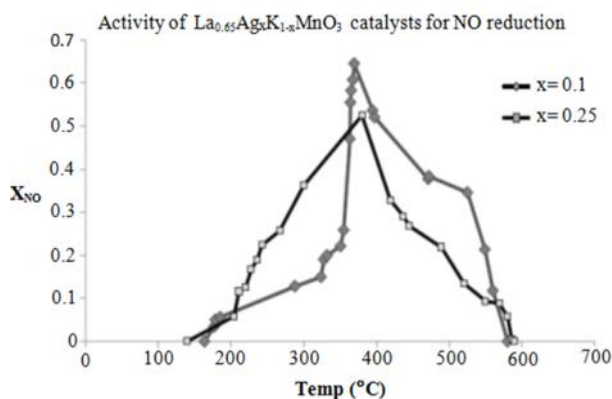


Figure 14. Effect of varying amount of K on NO conversion in $\text{La}_{0.65}\text{Ag}_x\text{K}_{1-x}\text{MnO}_3$ catalyst

better activity than the only silver doped catalyst. In a series of $\text{La}_{0.65}\text{Ag}_x\text{K}_{1-x}\text{MnO}_3$, the optimum substitution amount of K is for $x = 0.25$. The NO_x reduction with simultaneous soot oxidation is limited to 64% based on laboratory studies.

Acknowledgment

The authors would like to express his gratitude to the Department of Civil engineering and Chemical Engineering and Technology, Indian Institute of Technology (Banaras Hindu University) Varanasi, India; for their guidance and support.

References

- [1] Mwangi, J.K., Lee, W.-J., Chang, Y.-C., Chia-Chen, Y., Wang, L.-C. (2015). An Overview: Energy Saving and Pollution Reduction by Using Green Fuel Blends in Diesel Engines, *Applied Energy*, 159: 214-236.
- [2] Mishra, A., Prasad, R. (2015). Development of Highly Efficient Double-Substituted Perovskite Catalysts for Abatement of Diesel Soot Emissions. *Clean Technologies and Environmental Policy*. 17: 2337–2347.
- [3] Hoekman, S.K., Robbins, C. (2012). Review of the Effects of Biodiesel on NO_x Emissions, *Fuel Processing Technology*, 96: 237-249.
- [4] Cheng, Y., Liu, J., Zhao, Z., Wei, Y. (2017). Highly Efficient and Simultaneously Catalytic Removal of PM and NO_x from Diesel Engines with 3DOM $\text{Ce}_{0.8}\text{M}_{0.1}\text{Zr}_{0.1}\text{O}_2$ (M = Mn, Co, Ni) Catalysts, *Chemical Engineering Science*, 167: 219-228.
- [5] Huang, H., Liu, J., Sun, P., Ye, S. (2016). Study on the Simultaneous Reduction of Diesel Engine Soot and NO with Nano-CeO₂ Catalysts, *RSC Adv.*, 6: 102028.
- [6] Atribak, I., Bueno-López, A., García-García, A. (2008). Combined Removal of Diesel Soot Particulates and NO_x over CeO_2 - ZrO_2 Mixed Oxides. *Journal of Catalysis*. 259: 123–132.
- [7] Banús, E.D., Ulla, M.A., Miró, E.E., Milt, V.G. (2013). Structured Catalysts for Soot

Table 4. Comparison of activity of A-site substituted catalysts

Catalyst	T_i (°C)	X_{NO} (%)
LaMnO_3	204	45.34
$\text{La}_{0.65}\text{Ag}_{0.35}\text{MnO}_3$	154	53.28
$\text{La}_{0.65}\text{Ag}_{0.25}\text{K}_{0.1}\text{MnO}_3$	140	52.35
$\text{La}_{0.65}\text{Ag}_{0.1}\text{K}_{0.25}\text{MnO}_3$	130	64.48

- Combustion for Diesel Engines. *Diesel Engine-Combustion, Emissions and Condition Monitoring Application, Chapter-5*, 117–142.
- [8] Biamino, S., Fino, P., Fino, D., Russo, N., Badini, C. (2005). Catalyzed Traps for Diesel Soot Abatement: In Situ Processing and Deposition of Perovskite Catalyst. *Applied Catalysis B: Environmental*. 61: 297–305.
- [9] Yuvarajan, D., Ravikumar, J., Babu, M.D. 2016. Simultaneous Optimization of Smoke and NO_x Emissions in a Stationary Diesel Engine Fuelled with Diesel–Oxygenate Blends Using the Grey Relational Analysis in the Taguchi Method, *Anal. Methods*, 8: 6222
- [10] Bin, F., Song, C., Lv, G., Song, J., Gong, C., Huang, Q. (2011). La_{1-x}K_xCoO₃ and LaCo_{1-y}Fe_yO₃ Perovskite Oxides: Preparation, Characterization, and Catalytic Performance in the Simultaneous Removal of NO_x and Diesel Soot. *Industrial & Engineering Chemistry Research*. 50: 6660–6667.
- [11] Zwinkels, M.F.M., Järås, S.G., Menon, P.G., Griffin, T. (1993). Catalytic Materials for High-Temperature Combustion. *Catalysis Reviews*. 35(3): 319-358.
- [12] Cortés-Reyes, M., Herrera, M.C., Pieta, I.S., Larrubia, M.A., Alemana, L.J. (2016). In Situ TG-MS Study of NO_x and Soot Removal over LNT Model Catalysts, *Applied Catalysis A: General*, 523: 193-199.
- [13] Peña, M.A., Fierro, J.L.G. (2001). Chemical Structures and Performance of Perovskite Oxides. *Chemical Review*. 101(7): 1981–2018.
- [14] Liu, S., Wu, X., Weng, D., Ran, R. (2015). Ceria-based Catalysts for Soot Oxidation: A Review, *Journal of Rare Earths*, 33(6): 567-590.
- [15] Saracco, G., Scibilia, G., Iannibello, A., Baldi, G. (1996). Methane Combustion on Mg-doped LaCrO₃ Perovskite Catalysts. *Applied Catalysis B: Environmental*. 8: 229-244.
- [16] Wang, K., Qian, L., Zhang, L., Liu, H., Yan, Z. (2010). Simultaneous Removal of NO_x and Soot Particulates over La_{0.7}Ag_{0.3}MnO₃ Perovskite Oxide Catalysts. *Catalysis Today*, 158: 423–426.
- [17] Mishra, A., Prasad, R. (2014). Preparation and Application of Perovskite Catalysts for Diesel Soot Emissions Control: An Overview. *Catalysis Reviews: Science and Engineering*, 56(1): 57-81,
- [18] Matarrese, R., Morandi, S., Castoldi, L., Villa, P., Lietta, L. (2017). Removal of NO_x and Soot over Ce/Zr/K/Me (Me = Fe, Pt, Ru, Au) Oxide Catalysts, *Applied Catalysis B: Environmental*, 201: 318-330.
- [19] Saracco, G., Geobaldo, F., Baldi, G. (1999). Methane Combustion on Mg-doped LaMnO₃ Perovskite Catalysts. *Applied Catalysis B: Environmental*. 20: 277-288.
- [20] Xu, H., Yan, N., Qu, Z., Liu, W., Mei, J., Huang, W., Zhao, S. (2017). Gaseous Heterogeneous Catalytic Reactions over Mn-Based Oxides for Environmental Applications: A Critical Review, *Environ. Sci. Technol.*, 51 (16): 8879-8892.
- [21] Matarrese, R., Aneggi, E., Castoldi, L., Llorca, J., Trovarelli, A., Lietta, L. (2016). Simultaneous Removal of Soot and NO_x over K- and Ba-doped Ruthenium Supported Catalysts, *Catalysis Today*, 267: 119-129.
- [22] Ascaso, S., Moliner, R., Gálvez, M.E., Lazaro, M.J. (2013). Influence of the Alkali Promoter on the Activity and Stability of Transition Metal (Cu, Co, Fe) Based Structured Catalysts for the Simultaneous Removal of Soot and NO_x. *Topics in Catalysis*. 56: 493-498.
- [23] Zhu, R., Yan, Q., He, J., Cao, G., Ouyang, F. (2017). Simultaneous Removal of Soot and NO_x with Ru-Ir/TiO₂ Catalyst under Oxygen-Rich Condition, *Applied Catalysis A: General*, 541: 42-49.
- [24] Bueno-López, A., Lozano-Castelló, D., McCue, A.J., James A. (2017). NO_x Storage and Reduction over Copper-Based Catalysts. Part 3: Simultaneous NO_x and Soot Removal, *Applied Catalysis B: Environmental*, 198: 266-275.
- [25] Guo, X., Meng, M., Dai, F., Li, Q., Zhang, Z., Jiang, Z., Zhang, S., Huang, Y. (2013). NO_x-assisted Soot Combustion over Dually Substituted Perovskite Catalysts La_{1-x}K_xCo_{1-y}Pd_yO_{3-δ}, *Applied Catalysis B: Environmental*, 142-143: 278-289.
- [26] Bueno-López, A., Lozano-Castelló, D., Anderson, J.A. (2016). NO_x Storage and Reduction over Copper-Based Catalysts. Part 2: Ce_{0.8}M_{0.2}O₆ supports (M = Zr, La, Ce, Pr or Nd), *Applied Catalysis B: Environmental*, 198: 234-242.
- [27] Liu, J., Zhao, Z., Xu, C., Duan, A., Meng, T., Bao, X. (2007). Simultaneous Removal of NO_x and Diesel Soot Particulates over Nanometric La_{2-x}K_xCuO₄ Complex Oxide Catalysts, *Catalysis Today*, 119(1-4): 267-272.
- [28] Pecchi, G., Dinamarca, R., Campos, C.M., Garcia, X., Jimenez, R., Fierro, J.L.G. (2014). Soot Oxidation on Silver-Substituted LaMn_{0.9}Co_{0.1}O₃ Perovskites, *Industrial & Engineering Chemistry Research*, 53(24): 10090–10096.
- [29] Wang, K., Qian, L., Zhang, L., Liu, H., Yan, Z. (2010). Simultaneous Removal of NO_x and Soot Particulates over La_{0.7}Ag_{0.3}MnO₃

- Perovskite Oxide Catalysts, *Catalysis Today*, 158: 423–426.
- [30] Yang, R., Gao, Y., Wang, J., Wang, Q. (2014). Layered Double Hydroxide (LDH) Derived Catalysts for Simultaneous Catalytic Removal of Soot and NO_x, *Dalton Trans.*, 43: 10317.
- [31] Wang, Z., Lu, P., Zhang, X., Wang, L., Li, Q., Zhang, Z. (2015). NO_x Storage and Soot Combustion over Well Dispersed Mesoporous Mixed Oxides via Hydrotalcite-Like Precursors, *RSC Adv.*, 5: 52743.
- [32] Bockhorn, H., Kureti, S., Reichert, D. (2007). Study on the Mechanism of the Catalytic Conversion of NO_x and Soot into N₂ and CO₂ on Fe₂O₃ in Diesel Exhaust. *Topics in Catalysis*. 42-43(1-4): 283–286.
- [33] Liu, J., Zhao, Z., Xu, C., Duan, A. (2008). Simultaneous Removal of NO_x and Diesel Soot over Nanometer Ln-Na-Cu-O Perovskite-Like Complex Oxide Catalysts, *Applied Catalysis B: Environmental*, 78: 61–72.
- [34] Bosch, H., Janssen, F. (1998). Catalytic Reduction of Nitrogen Oxides: A Review of the Fundamentals and Technology. *Catalysis Today*. 2: 457-487.
- [35] Boyano, A., Lázaro, M.J., Cristiani, C., Maldonado-Hodar, F.J., Forzatti, P., Moliner, R. (2009). A Comparative Study of V₂O₅/AC and V₂O₅/Al₂O₃ Catalysts for the Selective Catalytic Reduction of NO by NH₃. *Chemical Engineering Journal*. 3:149-173.
- [36] Brosius, R., Arve, K., Groothaert, M.H., Martens, J.A. (2005). Adsorption Chemistry of NO_x on Ag/Al₂O₃ Catalyst for Selective Catalytic Reduction of NO_x Using Hydrocarbons. *Journal of Catalysis*. 231: 344–353.
- [37] Castoldi, L., Matarrese, R., Lietti, L., Forzatti, P. (2006). Simultaneous Removal of NO_x and Soot on Pt–Ba/Al₂O₃ NSR Catalysts. *Applied Catalysis B: Environmental*, 64: 25–34.
- [38] Trivedi, S., Prasad, R. (2016). Reactive Calcination Route for Synthesis of Active Mn–Co₃O₄ Spinel Catalysts for Abatement of CO–CH₄ Emissions from CNG Vehicles, *Journal of Environmental Chemical Engineering*, 4: 1017–1028.
- [39] Bin, F., Song, C., Lv, G., Song, J., Gong, C., Huang, Q. (2011). La_{1-x}K_xCoO₃ and LaCo_{1-y}Fe_yO₃ Perovskite Oxides: Preparation, Characterization, and Catalytic Performance in the Simultaneous Removal of NO_x and Diesel Soot, 2011, *Industrial & Engineering Chemistry Research*, 50(11): 6660–6667.
- [40] Zhao, B., Wang, R., Yang, X. (2009). Simultaneous Catalytic Removal of NO_x and Diesel Soot Particulates over La_{1-x}Ce_xNiO₃ Perovskite Oxide Catalysts, *Catalysis Communications*, 10(7): 1029-1033.
- [41] Li, Z., Meng, M., Zha, Y., Dai, F.F., Hu, T., Xie, Y., Zhang, J. (2012). Highly Efficient Multifunctional Dually-Substituted Perovskite Catalysts La_{1-x}K_xCo_{1-y}Cu_yO_{3-δ} used for Soot Combustion, NO_x Storage and Simultaneous NO_x-Soot Removal, *Applied Catalysis B: Environmental*, 121-122: 65-74.